

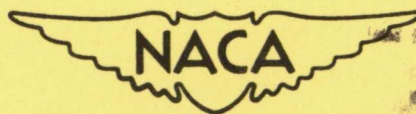
# NATIONAL ADVISORY COMMITTEE FOR AERONAUTICS

TECHNICAL NOTE 3345

## ARRANGEMENT OF FUSIFORM BODIES TO REDUCE THE WAVE DRAG AT SUPERSONIC SPEEDS

By Morris D. Friedman and Doris Cohen

Ames Aeronautical Laboratory  
Moffett Field, Calif.



Washington

November 1954

THIS DOCUMENT ON LOAN FROM THE FILES OF

NATIONAL ADVISORY COMMITTEE FOR AERONAUTICS  
LIBRARY  
Moffett Field, Calif.

RESEARCH AND TECHNICAL SERVICES

RESEARCH AND TECHNICAL SERVICES OF AERONAUTICS  
Moffett Field, Calif.

NATIONAL ADVISORY COMMITTEE FOR AERONAUTICS  
Moffett Field, Calif.  
November 1954

# NATIONAL ADVISORY COMMITTEE FOR AERONAUTICS

---

## TECHNICAL NOTE 3345

---

### ARRANGEMENT OF FUSIFORM BODIES TO REDUCE THE

### WAVE DRAG AT SUPERSONIC SPEEDS<sup>1</sup>

By Morris D. Friedman and Doris Cohen

#### SUMMARY

Using linearized slender-body theory and reverse-flow theorems, the wave drag of a system of fusiform bodies at zero angle of attack and supersonic speeds is studied to determine the effect of varying the relative location of the component parts. The investigation is limited to two-body and three-body arrangements of Sears-Haack minimum-drag bodies. It is found that in certain arrangements the interference effects are beneficial, and may even result in the two- or three-body system having no more wave drag than that of the principal body alone. The most favorable location appears to be one in which the maximum cross section of the auxiliary body is slightly forward of the Mach cone from the tail of the main body. The least favorable is the region between the Mach cone from the nose and the forecone from the tail of the main body.

#### INTRODUCTION

When an airplane is to be equipped with external fuel tanks or prominent nacelles, the effect on the drag will vary widely with the location of such auxiliary bodies relative to the other parts of the airplane. In reference 1, calculations were made of the theoretical interference drag between the fusiform bodies of some typical arrangements, under the conditions of supersonic speed and zero angle of attack. Later developments in linear theory have provided a simpler method of performing such calculations, and the present paper is a revision of reference 1 to take advantage of these developments. Both reference 1 and the present work are largely based on suggestions of R. T. Jones.

Two arrangements will be considered - a two-body combination, as when one body is suspended beneath another, and a laterally symmetric

---

<sup>1</sup>Supersedes NACA RM A51I20, "Arrangement of Bodies of Revolution in Supersonic Flow to Reduce Wave Drag" by Morris D. Friedman, 1951.

---

three-body arrangement. The radial and streamwise displacements of the auxiliary body or bodies relative to the main one will constitute the parameters of the investigation. The calculations will be made for combinations of Sears-Haack minimum-drag bodies (refs. 2 and 3), but the method of analysis is applicable to any slender shapes for which the pressure fields are known. In particular, it may be mentioned that the main body and auxiliary bodies need not be similar.

## ANALYSIS

### Reversed-Flow Theory

A basic condition of the analysis is that the bodies be slender enough so that they may be represented by a linear distribution of singularities - sources for a body of revolution, or higher-order singularities for cambered bodies - of which the strength may be determined from local conditions. In that case, simultaneously reversing the direction of flow and the sign of the source strength associated with a given isolated body does not change the shape of the body, and the reversed-flow theorems of reference 4, which are stated in terms of source distributions, may be applied to the bodies themselves. However, the streamlines at a distance from the body are altered, so that it is not generally to be expected that the theorems would be applicable to a system of bodies of prescribed geometry. The location of the individual bodies of the system in the streamlines of the other bodies has the effect of introducing additional camber into the boundary conditions and thereby modifying the equivalent distribution of singularities. Calculations made to investigate the effect of such induced camber on the drag of slender bodies indicate that the magnitude is not likely to be any significant fraction of the thickness drag.<sup>2</sup> The additional drag introduced by the induced camber will therefore be ignored. With this simplification, the drag of a system of slender bodies may be said to remain unchanged when the direction of motion is reversed.

In the present calculations, in which each of the bodies is symmetrical fore and aft, the first consequence of the reversibility property is that only rearward (or forward) displacements of the auxiliary bodies relative to the main body need be considered.

The reversibility property also leads to the possibility of combining the pressure fields for forward and reverse flow before computing the drag, and taking half the result as the drag in either direction.

---

<sup>2</sup>For example, the drag due to parabolic camber of a line of sources corresponding to a Sears-Haack body is  $\frac{16}{3}(M^2 - 1)h^2$  times the drag of of the uncambered body,  $h$  being the maximum camber in percent of body length.

---

This point may be demonstrated as follows:

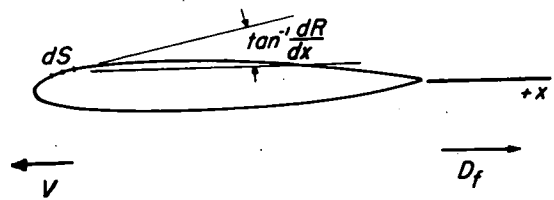
Let  $dR/dx$  be the local inclination of any element of surface area (of a body of revolution) to the stream and  $c_{p_f}$  be the pressure coefficient at the centroid of the element when the body is in forward motion. Then the corresponding element of drag (sketch (a)) is simply (to the first order)

$$q c_{p_f} dR/dx dS$$

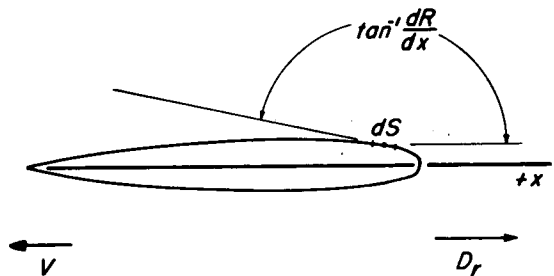
where  $q$  is the free-stream dynamic pressure and  $S$  is the surface area. Now, let the body be reversed on the  $x$  axis (sketch (b)) and flow tail foremost. At the previously considered element of area a new pressure coefficient  $c_{p_r}$  will result; the slope  $dR/dx$  will merely be reversed in sign. The sum of the two elements of drag will be

$$dD_f + dD_r = q \left( c_{p_f} - c_{p_r} \right) \left( \frac{dR}{dx} \right)_f dS \quad (1)$$

where the subscript  $f$  refers to quantities measured in forward motion and  $r$  to quantities in rearward motion. The total combined drag is the integral of this quantity, and is twice the drag of the body traveling in either direction.



Sketch (a)



Sketch (b)

The foregoing device, similar to one first suggested in reference 5, results in considerable mathematical simplification in many cases. Thus, the argument of reference 6 that in the combined flow field the drag of one wing due to the field of another is equal to that of the second due to the field of the first can be extended to apply to systems of slender bodies under the conditions outlined above. Then only one calculation of the interference drag need be made for each pair of bodies; for example, in the present analysis only the drag of the auxiliary body due to the combined pressure field of the main body will be calculated.

### Pressure Field of a Sears-Haack Body

In the examples to be worked in this paper, all bodies will be closed bodies of revolution having individually the form for minimum theoretical wave drag for given length and volume.<sup>3</sup> This shape (refs. 2 and 3) is given by

$$R^2(x) = c(l^2 - x^2)^{3/2} \quad (2)$$

(See Appendix for a list of symbols.) The flow about one such body can be calculated as the flow due to a distribution of sources and sinks along the body axis, the source strength  $f(x)$  being related to the body geometry by the equation (ref. 7)

$$2\pi f(x) = V \frac{dSc}{dx} = \pi V \frac{dR^2}{dx} \quad (3)$$

The pressure coefficient near the body is given to the first order (see ref. 8) by the relation

$$c_p = - \frac{2u}{V} - \left( \frac{v}{V} \right)^2 \quad (4a)$$

in which  $u = \partial\phi/\partial x$  is the streamwise component of the perturbation velocity and  $v = \partial\phi/\partial r$  the radial component. Inasmuch as the latter component falls off with distance from the body as  $1/r$  and its contribution to the pressure decreases with  $1/r^2$ , it may be possible to neglect the second term in  $c_p$  in computing the interference drag. It will be shown by a numerical example that this simplification is in fact permissible in the present investigation. At the surface of the body, the ratio  $v/V$  is, to first order, the streamwise slope of the body and, in the case of the symmetrical bodies under consideration, the integration for the drag will result in canceling out all effects

---

<sup>3</sup>In a recent analysis, Conrad Renneman, Jr., of the NACA has found that the form of a body of revolution for minimum drag in the field of a larger body is not significantly different from the Sears-Haack shape, nor can any important reduction in the theoretical wave drag be achieved by modifying the shape of the body from the Sears-Haack shape.

---

of the radial component of velocity. Thus it is sufficient for our purpose to retain only the linear term in equation (4a), writing

$$c_p \approx - \frac{2u}{V} \quad (4b)$$

From reference 7,

$$\frac{\partial \phi}{\partial x} = - \int_{\text{nose}}^{x-\beta r} \frac{f'(\xi) d\xi}{\sqrt{(x-\xi)^2 - \beta^2 r^2}} \quad (5)$$

From equations (2) and (3),  $f'(\xi)$  is in the present case

$$- \frac{3}{2} Vc \frac{l^2 - 2\xi^2}{\sqrt{l^2 - \xi^2}}$$

and

$$c_p \approx -3c \int_{-l}^{x-\beta r} \frac{(l^2 - 2\xi^2) d\xi}{\sqrt{(l^2 - \xi^2)[(x-\xi)^2 - \beta^2 r^2]}} \quad (6)$$

It should be remarked that for  $\xi > l$  the integrand vanishes, and that  $c_p$  is zero when  $x - \beta r < -l$ .

The integration in equation (6) yields three different expressions, depending on whether

$$\beta r - l < x < l - \beta r \quad (\text{Region I})$$

$$x - \beta r < l < x + \beta r \quad (\text{Region II})$$

or

$$l < x - \beta r \quad (\text{Region III})$$

The three regions defined above are shown in figure 1. The expressions

for the approximate pressure coefficient are

Region I

$$c_{p_I} \simeq -3\pi c \left[ \frac{l^2 + 2\beta r(l-x) - 2x^2}{\sqrt{(l+\beta r)^2 - x^2}} K_0(k_1) - \sqrt{(l+\beta r)^2 - x^2} E_0(k_1) + 2x\Lambda_0(\psi_1, k_1) \right]$$

$$k_1 = \sqrt{\frac{(l-\beta r)^2 - x^2}{(l+\beta r)^2 - x^2}} \quad \psi_1 = \sin^{-1} \sqrt{\frac{l+\beta r+x}{2l}} \quad (7)$$

Region II

$$c_{p_{II}} \simeq -3\pi c \left[ \frac{l(l+2\beta r-2x)}{2\sqrt{l\beta r}} K_0(k_2) - 2\sqrt{l\beta r} E_0(k_2) + 2x\Lambda_0(\psi_2, k_2) \right]$$

$$k_2 = \sqrt{\frac{x^2 - (\beta r - l)^2}{4l\beta r}} \quad \psi_2 = \sin^{-1} \sqrt{\frac{2l}{l+\beta r+x}} \quad (8)$$

Region III

$$c_{p_{III}} \simeq 3\pi c \left[ \frac{(x-\beta r)^2}{\sqrt{x^2 - (\beta r - l)^2}} K_0(k_3) + \sqrt{x^2 - (\beta r - l)^2} E_0(k_3) - 2x\Lambda_0(\psi_3, k_3) \right]$$

$$k_3 = \sqrt{\frac{4l\beta r}{x^2 - (\beta r - l)^2}} \quad \psi_3 = \sin^{-1} \sqrt{\frac{l+x-\beta r}{l+x+\beta r}} \quad (9)$$

The quantities  $K_0$ ,  $E_0$  and  $\Lambda_0$  are defined in Appendix A and tabulated in reference 9;  $\Lambda_0$  is tabulated also in reference 10.

The magnitude of the approximate pressure coefficient at the surface of a body of fineness ratio 10, as given by equation (7), is plotted in figure 2(a), together with the more accurate values obtained by the use of equation (4a). It is apparent that the difference, in the case of so slender a body, is not great and, as previously noted, will diminish rapidly with distance.

An isometric sketch of the pressure coefficient calculated by equation (4b) is shown in figure 2(b). Of particular interest is the

logarithmic infinity along the Mach cone from the tail of the body. Except at the body itself, the pressure is finite everywhere else and goes smoothly through the forecone from the tail, in spite of the change in the form of its mathematical expression.

### Combined Pressure Field

If now the body is reversed in heading and the resulting pressure field subtracted from that given above, the combined pressure field is found as

$$\bar{c}_p(x) = c_p(x) - c_p(-x) \quad (10)$$

because of the fore-and-aft symmetry of the body. The various regions of the combined field are shown in figure 3.

It is seen from figure 3 that there is only one region in which any possibility of further mathematical simplification appears. In this region (where Region I and Region I of the reversed field overlap) we have to consider

$$\bar{c}_{p_I} = c_{p_I}(x) - c_{p_I}(-x) \quad (11)$$

Through the relation (ref. 10, p. 36)

$$\Lambda_0(\psi, k) + \Lambda_0(\bar{\psi}, k) = 1 + k'^2 K_0 \sin \psi \sin \bar{\psi}$$

when

$$\tan \psi \tan \bar{\psi} = \frac{1}{k}$$

equation (11) reduces to

$$\bar{c}_{p_I} = -6\pi c x \quad (12)$$

Thus, the pressure gradient of the combined field is a constant in the neighborhood of the body, as specified in reference 6 for minimum wave drag with a given volume.<sup>4</sup>

---

<sup>4</sup>Although reference 6 deals specifically with thin wings, it is readily shown that the same considerations hold for slender bodies under the assumptions used herein.

---



### Calculation of the Wave Drag

As previously indicated, it is proposed in calculating the drag to ignore the drag introduced by the curvature of the flow due to adjacent bodies, and therefore to replace each body by the equivalent source distribution in a uniform stream. If, following this course, we consider the entire flow field to be essentially the result of the superposition of the fields of the individual bodies, we have to compute

(a) one-half the drag of each body in its own combined pressure field,

(b) the drag of each auxiliary body in the combined field of the main body, and

(c) the drag of one auxiliary body in the field of the other, if more than one auxiliary body is included. It may be seen that the drag of the second body in the field of the first is taken care of by the factor of 2 introduced by the use of the combined pressure field.

If equation (1) is applied to a body of revolution, the total drag in combined flow may be written

$$\bar{D} = 2\pi q \int_{-l}^{+l} \bar{c}_p R \frac{dR}{dx} dx = \pi q \int_{-l}^{+l} \bar{c}_p \frac{dR^2}{dx} dx \quad (13)$$

and, for the Sears-Haack bodies,

$$\frac{dR^2}{dx} = -3cx \sqrt{l^2 - x^2} \quad (14)$$

The drag of each body due to its own pressure field is then one-half that obtained by substituting from equations (12) and (14) in equation (13), or

$$\begin{aligned} D_O &= 9\pi^2 qc^2 \int_{-l}^{+l} x^2 \sqrt{l^2 - x^2} dx \\ &= \frac{9}{8} \pi^3 q l^4 c^2 \end{aligned} \quad (15)$$

or, since the maximum cross-sectional area is, from equation (2),

$$S_F = \pi c l^3 \quad (16)$$

the drag in terms of frontal area is

$$D_0 = \frac{9}{8} \pi \frac{S_F^2}{l^2} q \quad (17)$$

which is in agreement with the value given in reference 2.

The interference drag is calculated by substituting in equation (13) the pressure coefficient associated with one body and the value of  $dR^2/dx$  associated with the other. Considering first a two-body combination, we may take the origin of coordinates at the center of one, which will be designated the "main" body, and let the center of the auxiliary body be displaced from it a distance  $x_0$  downstream and a distance  $r_0$  laterally or vertically. Then, if for a first approximation the pressure field of the main body is assumed not to vary significantly in the distance between the axis of the auxiliary body and its surface, the values of  $\bar{c}_p$  are obtained from equations (12), (8), and (9) by letting  $r = r_0$ . Equation (14) is modified to take into account the displacement of the auxiliary body:

$$\frac{dR^2}{dx} = -3c_1(x - x_0)\sqrt{l_1^2 - (x - x_0)^2} \quad (18)$$

and the geometric characteristics of the second body are used to determine  $c_1$  and  $l_1$ .

It is immediately apparent that if the auxiliary body lies entirely within Region I (fig. 3), the value of  $\bar{c}_p$ , and therefore of the drag, is independent of  $r_0$ . In fact, since the pressure gradient is a constant throughout the region, the drag is entirely independent of position so long as the body remains within Region I. The interference drag in this case is simply

$$D_1 = \frac{9}{8} \pi^3 q l_1^4 c c_1 \quad (19)$$

or, more generally,  $D_1/q$  equals the pressure gradient  $6\pi c$  times the volume of the auxiliary body, regardless of its shape.

In Region II, however, the pressure gradient changes from negative to positive (see fig. 2(b)) and a small body placed so as to take advantage of this buoyancy would conceivably experience a negative interference drag, or thrust, which would act to reduce the total drag of the combination. Substitution of  $c_{p_{II}}$  and, when required,  $c_{p_{III}}$  in equation (13) results in integrals which can be evaluated only numerically. We therefore proceed at this point to the consideration of numerical examples.

## NUMERICAL CALCULATIONS

For an exploratory investigation, the simple case of two bodies of fineness ratio 10, the small body having one-half the length of the main body, was chosen. This combination is derived by assigning the following values to the parameters of the problem:

$$\begin{aligned} c &= 0.01 & l &= 1 \\ c_1 &= .02 & l_1 &= 1/2 \end{aligned}$$

In compressible flow, the Mach number and cross-stream dimensions always enter together in the form of  $\beta r_0$ . Three values of  $\beta r_0/l$  have been selected: 0.25, 0.5, and 1.0. The effect of streamwise displacement is investigated to a distance equal to the length of the larger body.

The interference between the two outer bodies of a three-body configuration was calculated in the case of  $\beta r_0/l = 0.25$ , the only case, because of the limited zones of influence at supersonic speeds, in which any such interference takes place. The interference drag was found to be negligible. The results to be presented are therefore equally applicable to the two-body or three-body arrangement, only a factor of two in the interference drag being required.

## RESULTS AND DISCUSSION

The variation of the interference drag with streamwise and radial displacement is shown in figure 4. Because of the symmetry of the curves, the effects of rearward displacement only are presented. The sketches indicate, for  $M = \sqrt{2}$ , the relative positions of the bodies at which the interference is greatest. The anticipated favorable interference is observed when the small body is situated astride the region of negative pressure gradient just ahead of the Mach wave from the stern of the large body. A second case of favorable interference is seen in figure 4(c) when the pressure field of the large body acts only on the rear of the small body, resulting in unopposed thrust. This situation, in the case of forward displacement of the small body, is also responsible for the dip in the interference drag at  $x_0/l = 0.7$  when  $\beta r_0/l = 0.5$ , and reinforces the minimum in the neighborhood of  $x_0/l = 0.95$  when  $\beta r_0/l = 0.25$ .<sup>5</sup>

---

<sup>5</sup>The situation described actually takes place at  $x_0/l = -0.5$  and  $-0.75$  in the two cases, but the general slope of the curve due to the proximity of stronger minimums causes a shift of the secondary dips.

In the corresponding cases of rearward displacement, the thrust is the result of the location of the rear of the large body in a positive gradient due to the small body, but there is a more involved balance of forces and the net result is not as easily foreseen. As is to be expected, the maximum benefit obtainable decreases with increasing radial separation of the bodies. The maximum penalty is incurred when the auxiliary body is added between the Mach cone from the nose and the fore-cone from the tail of the main body.

In figures 5 and 6 the wave drag coefficient based on total frontal area is shown for two-body and three-body arrangements. These figures indicate that in frictionless potential flow it might be possible to increase the volume by as much as 25 percent (three-body arrangement) and at the same time actually decrease the wave drag. In practice, of course, the additional friction drag might easily nullify any such gain. Nevertheless, if there are to be auxiliary bodies, the importance of their relative positions seems clear.

Ames Aeronautical Laboratory  
National Advisory Committee for Aeronautics  
Moffett Field, Calif., Sept. 8, 1954

## APPENDIX

## SYMBOLS

$c$	coefficient containing body dimensions, $\frac{R_{\max}^2}{l^3}$
$c_1$	value of $c$ for auxiliary body
$C_{D_W}$	wave-drag coefficient, $\frac{D_W}{qS_F}$
$C_{D_i}$	interference drag coefficient, $\frac{D_i}{qS_F}$
$c_p$	local pressure coefficient
$c_{p_f}$	pressure coefficient in forward motion
$c_{p_r}$	pressure coefficient in reversed motion
$\bar{c}_p$	pressure coefficient in "combined" motion, $c_{p_f} - c_{p_r}$
$D_W$	wave drag
$D_O$	wave drag of isolated body
$D_i$	interference drag
$D_f$	wave drag in forward motion
$D_r$	wave drag in reversed motion
$\bar{D}$	combined wave drag, $D_f + D_r$
$E_O$	$\frac{2}{\pi}$ times complete elliptic integral of the second kind
$f$	source strength
$k$	modulus of elliptic integrals (with subscripts to indicate different values)
$k'$	complementary modulus, $\sqrt{1 - k^2}$
$K_O$	$\frac{2}{\pi}$ times complete elliptic integral of the first kind

$l$	half-length of body
$l_1$	half-length of auxiliary body
$M$	free-stream Mach number
$q$	free-stream dynamic pressure
$r$	radial coordinate, measured from body axis
$r_0$	radial coordinate of center of auxiliary body
$R$	local radius of body (function of $x$ )
$R_{\max}$	radius of body at maximum cross section
$S$	surface area
$S_c$	cross-sectional area
$S_F$	maximum cross section, or frontal area
$u$	streamwise component of perturbation velocity
$v$	radial component of perturbation velocity
$V$	free-stream velocity
$x$	streamwise coordinate
$x_0$	streamwise coordinate of center of auxiliary body
$\beta$	$\sqrt{M^2 - 1}$
$\Lambda_0(\psi, k)$	Heumann's elliptic function, $E_0(k)F(\psi, k') + K_0(k)E(\psi, k') - K_0(k)F(\psi, k')$ , tabulated in references 9 and 10
$\xi$	streamwise coordinate of source
$\phi$	perturbation velocity potential
$\psi$	argument of incomplete elliptic integrals in $\Lambda_0$ (with subscripts to denote various values)

## REFERENCES

1. Friedman, Morris D.: Arrangement of Bodies of Revolution in Supersonic Flow to Reduce Wave Drag. NACA RM A51I20, 1951.
2. Sears, William R.: On Projectiles of Minimum Wave Drag. Quart. Appl. Math., vol. IV, no. 4, Jan. 1947, pp. 361-366.
3. Haack, W.: Projectile Shapes for Smallest Wave Drag. Brown Univ., Grad. Div. Appl. Math., Trans. A9-T-3, 1948.
4. Hayes, Wallace D.: Linearized Supersonic Flow. (Thesis) North Amer. Aviation, Inc., Rep. AL-222, 1947.
5. Munk, M. M.: The Reversal Theorem of Linearized Supersonic Airfoil Theory. Jour. Appl. Phys., vol. 21, no. 2, Feb. 1950, pp. 159-161.
6. Jones, Robert T.: Theoretical Determination of the Minimum Drag of Airfoils at Supersonic Speeds. Jour. Aero. Sci., vol. 19, no. 12, Dec. 1952, pp. 813-822.
7. von Kármán, Th.: The Problem of Resistance in Compressible Fluids. GALCIT pub. no. 75, 1936. (From R. Acad. D'Italia; cl. scie., fis. mat. e nat., vol. XIV, 1936)
8. Lighthill, M. J.: Methods for Predicting Phenomena in the High-Speed Flow of Gases. Jour. Aero. Sci., vol. 16, no. 2, Feb. 1949, pp. 69-83.
9. Heumann, Carl: Tables of Complete Elliptic Integrals. Jour. Math. and Phys., vol. 19-20, 1940-41, pp. 127-206.
10. Byrd, Paul F., and Friedman, Morris D.: Handbook of Elliptic Integrals for Engineers and Physicists. Springer-Verlag (Berlin), 1954.

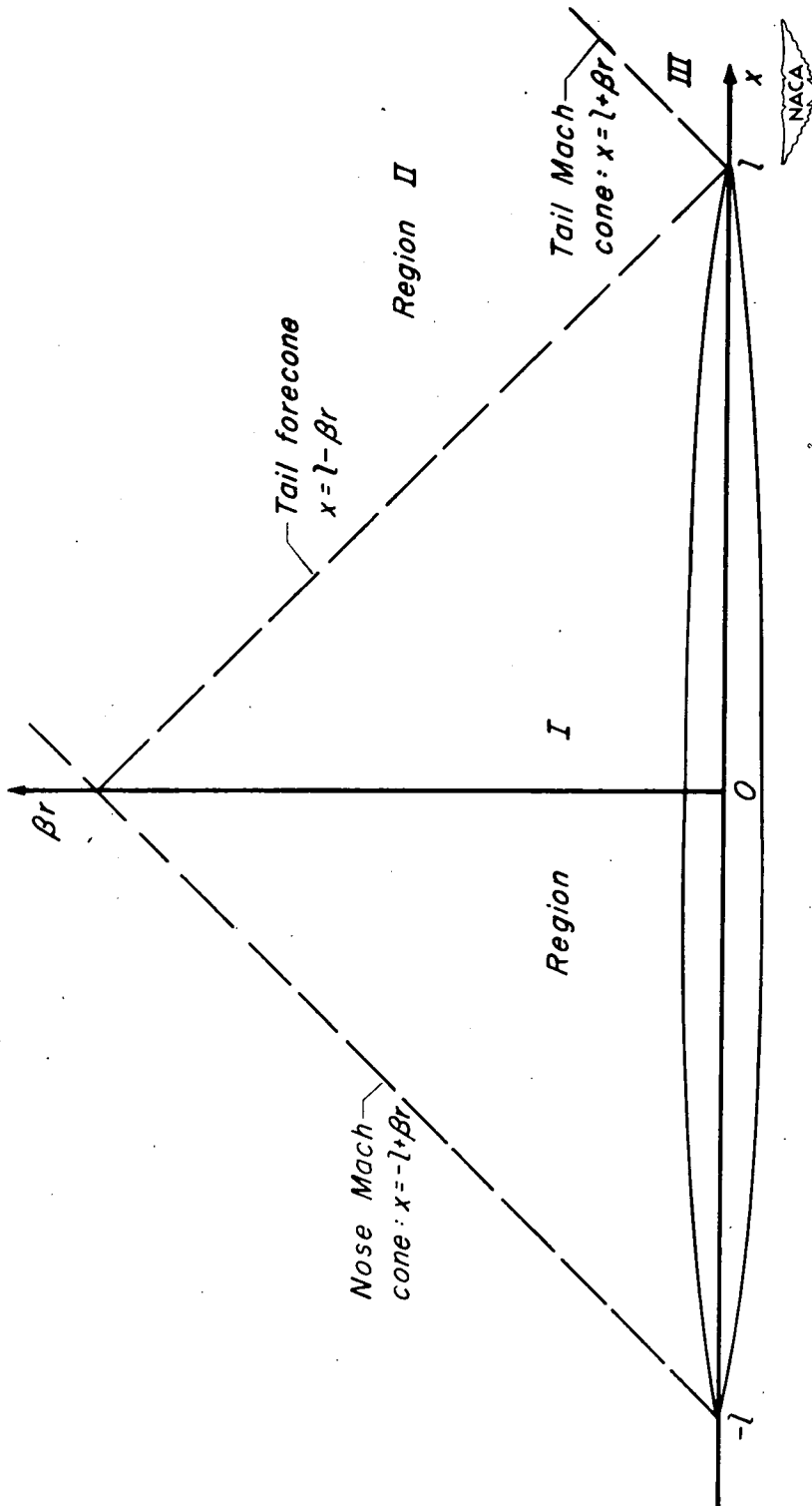
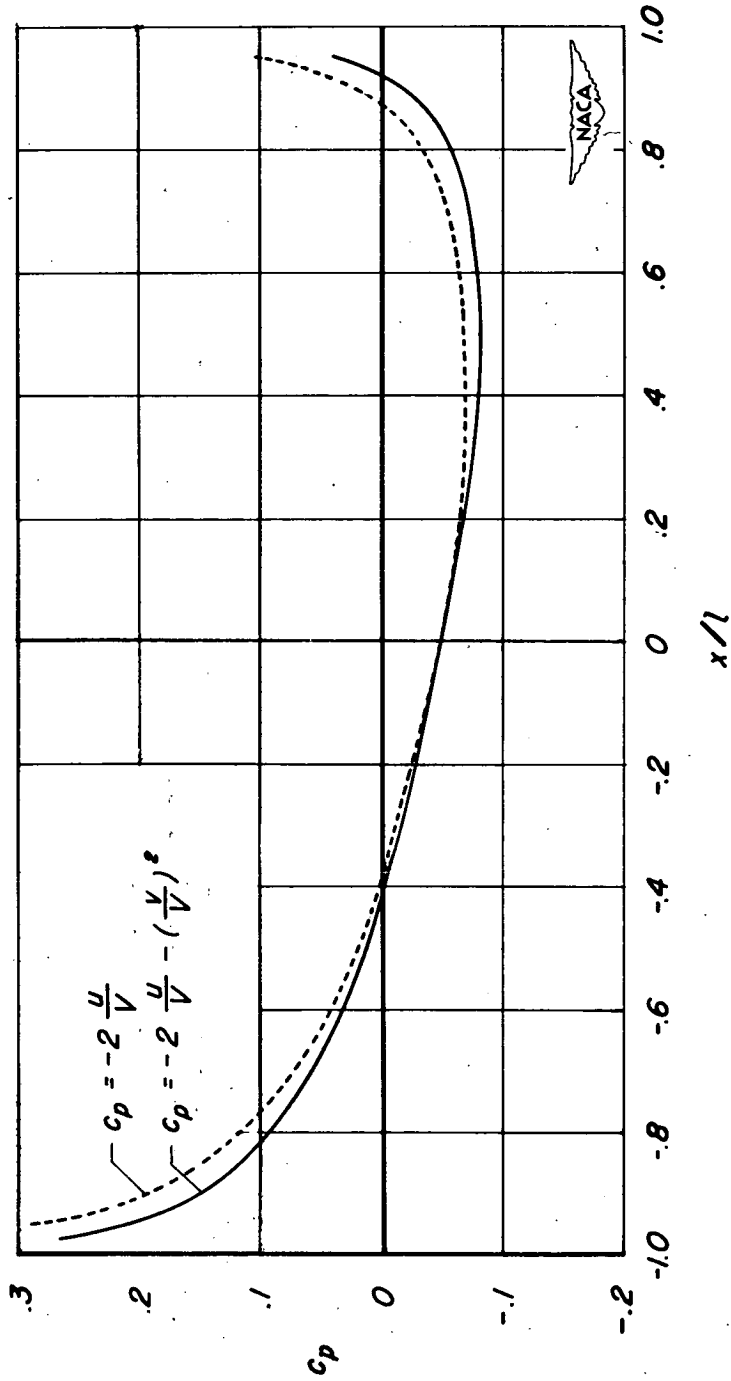


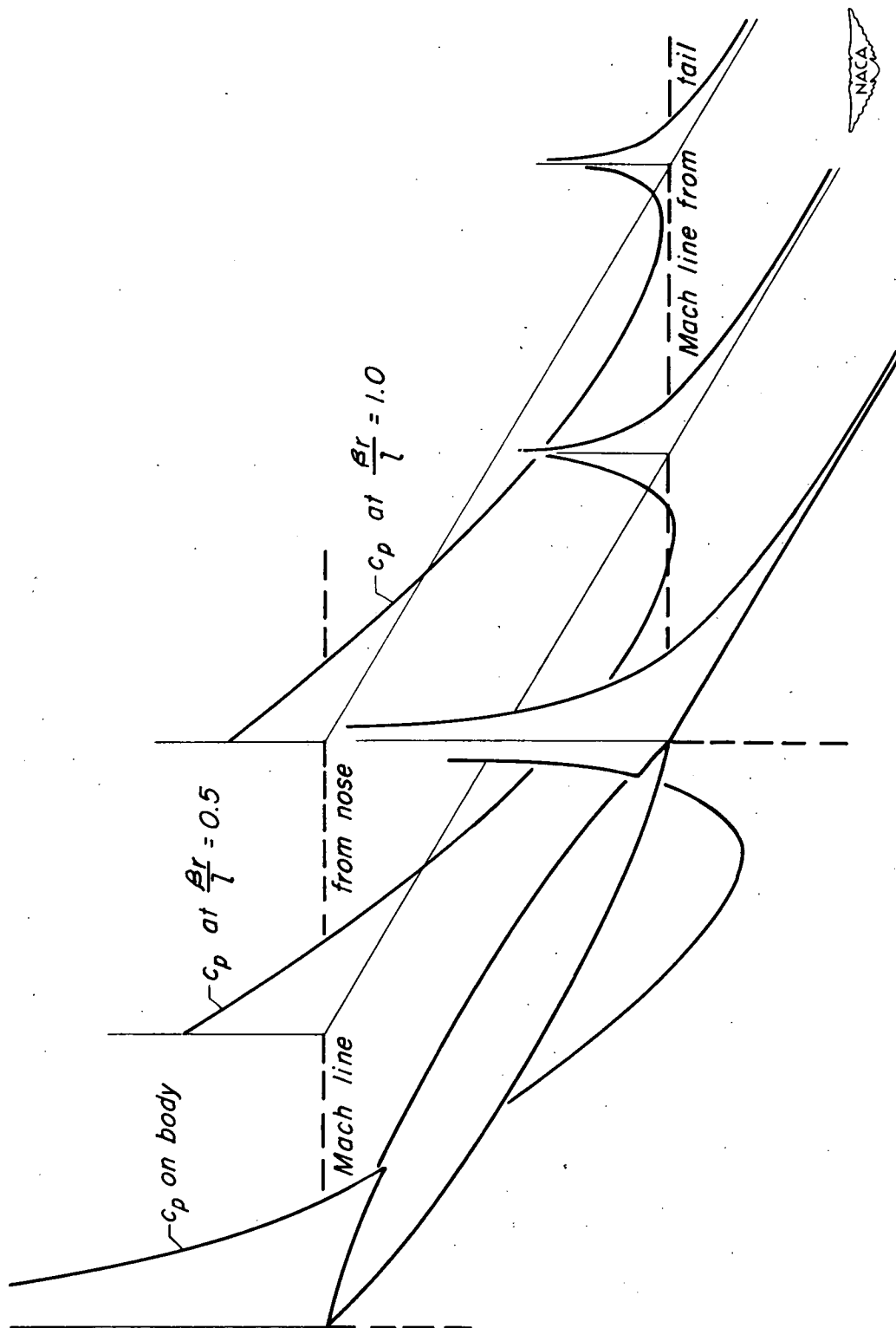
Figure 1. - Regions in pressure field around isolated Sears-Haack body.





(a) Effect of  $v^2$  term on the value of  $c_p$  on the body.

Figure 2.- Pressure coefficient, Sears-Haack body, fineness ratio 10.



(b) Isometric sketch of the pressure distribution in the field surrounding a single body.

Figure 2. - Concluded.

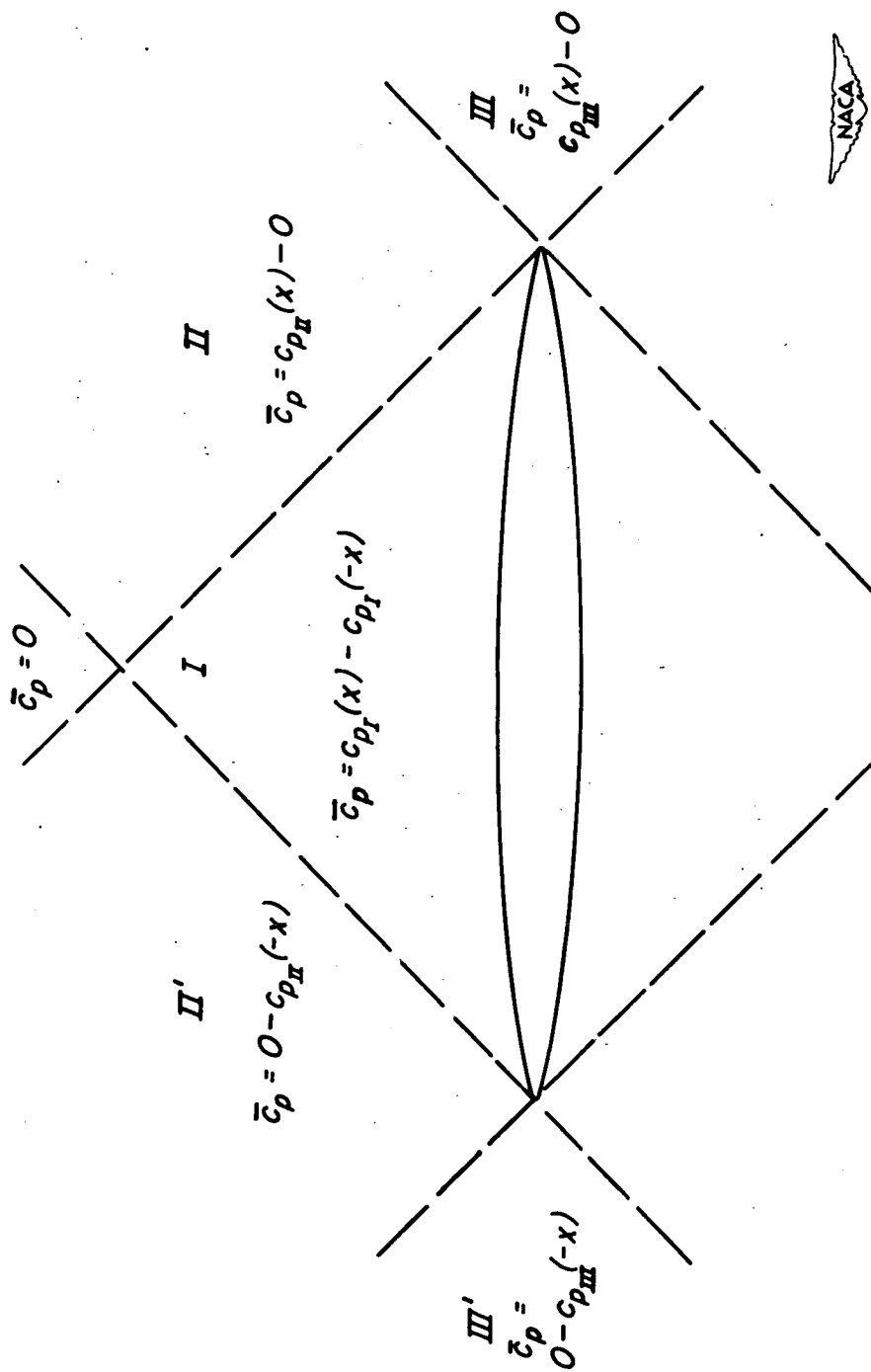
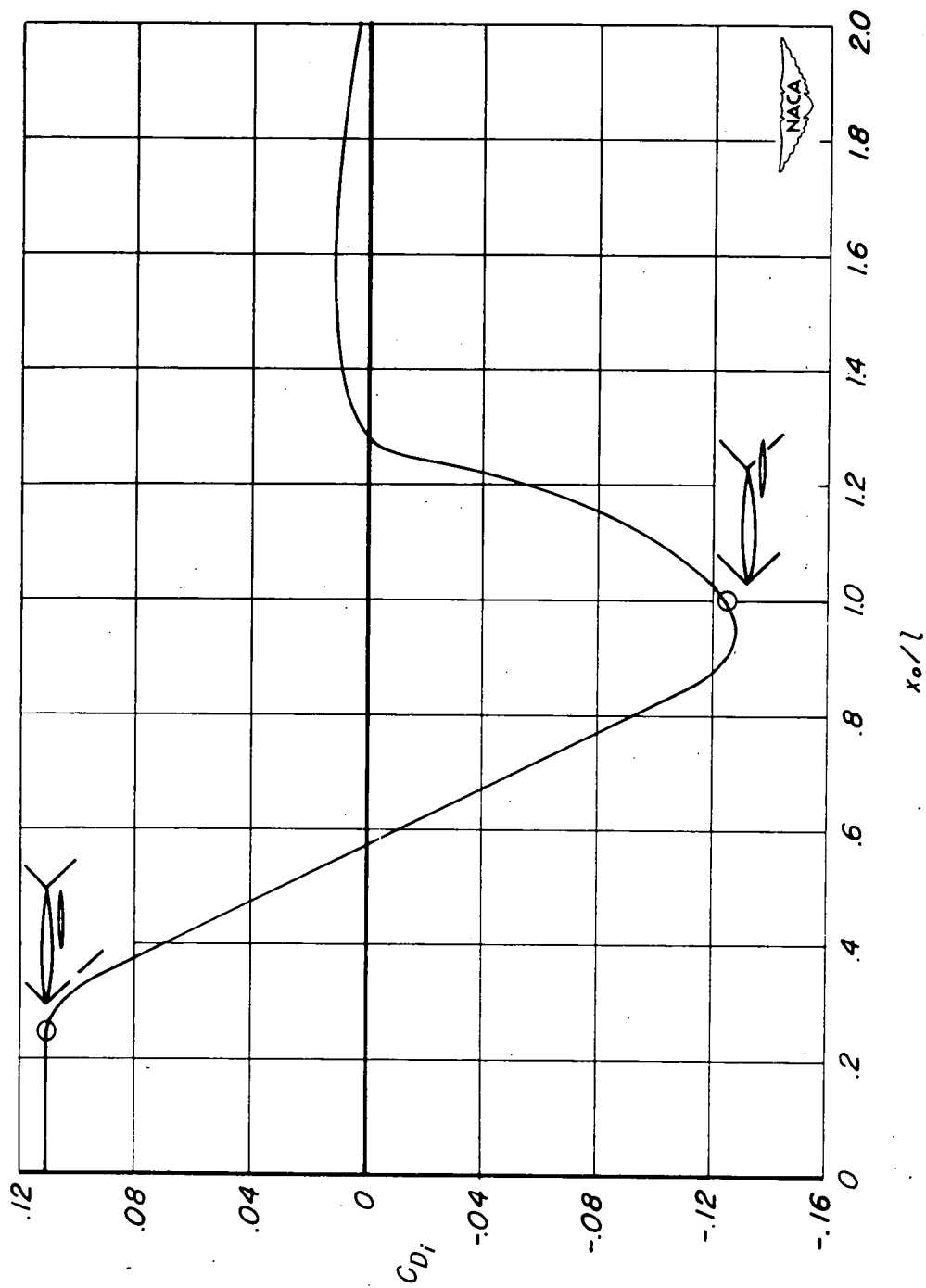
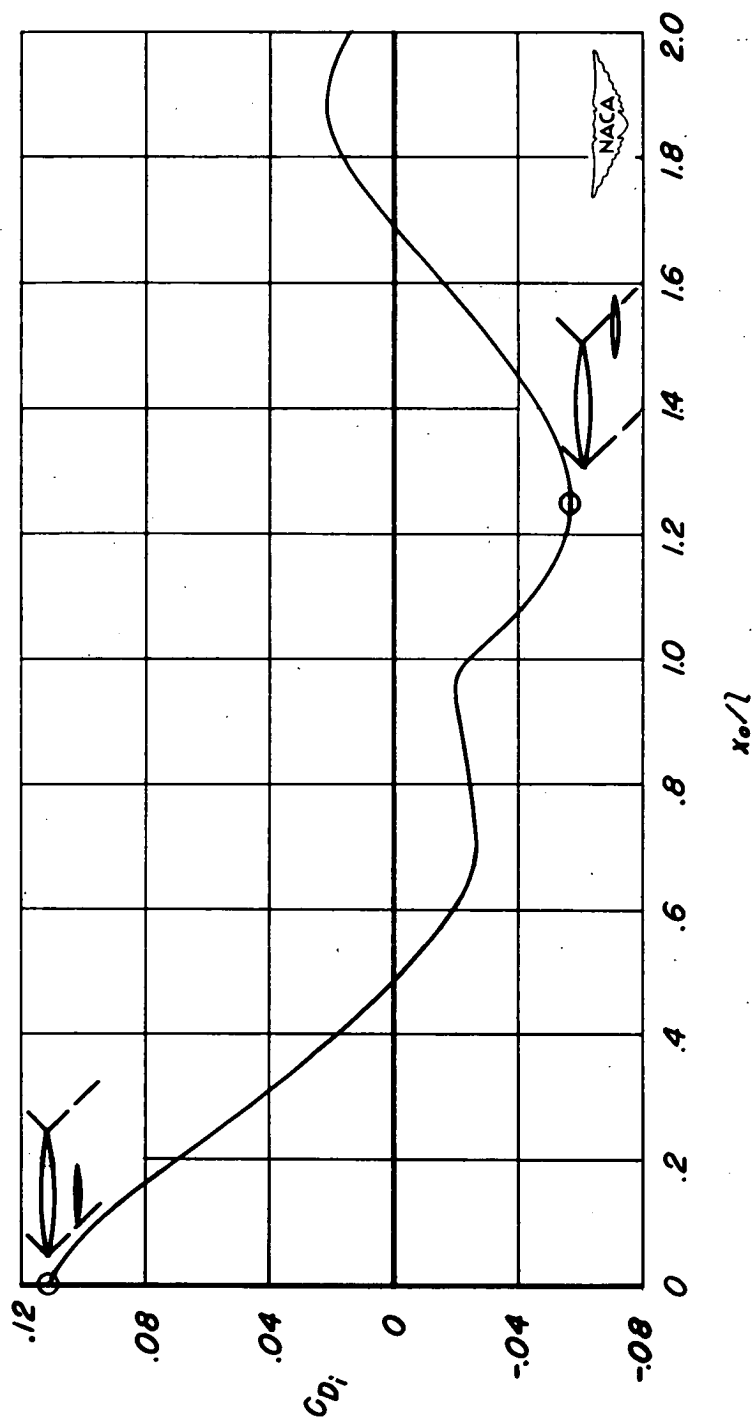


Figure 3. - Various regions in combined pressure field of a single body.



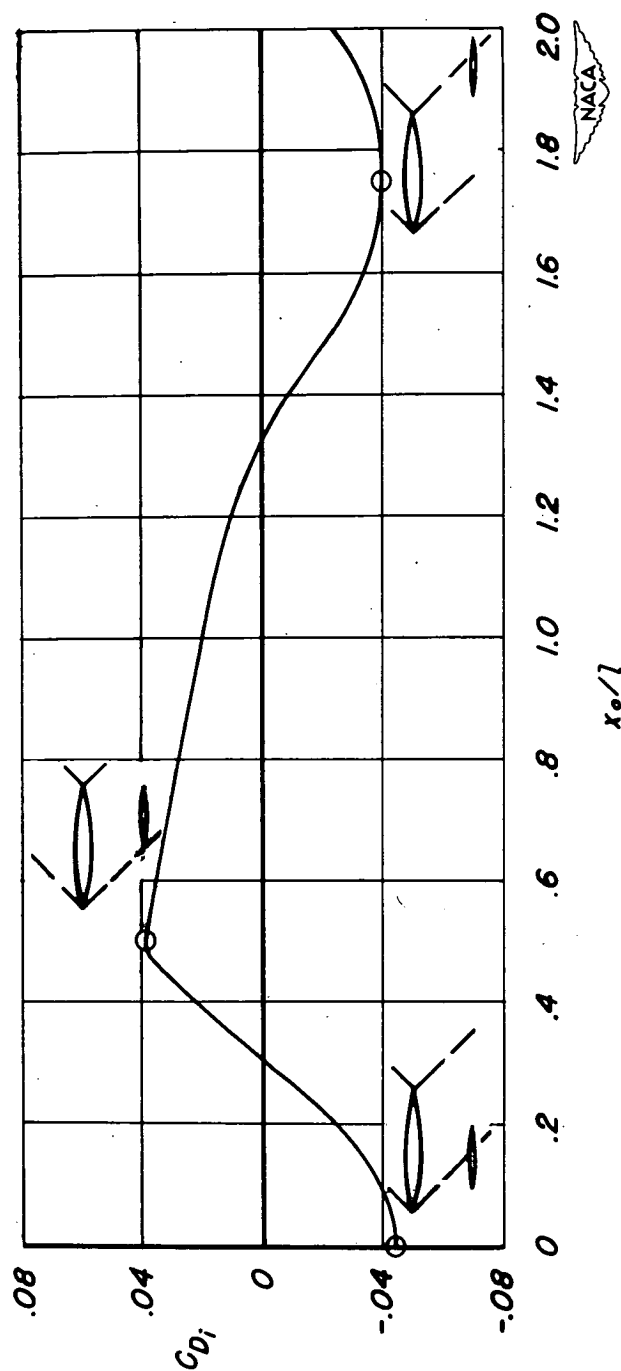
(a)  $\beta r_0/l = 0.025$

Figure 4. - Interference drag per unit added frontal area.



(b)  $\beta_o/l = 0.50$

Figure 4. - Continued.



(c)  $\beta r_o/l = 1.00$

Figure 4. - Concluded.

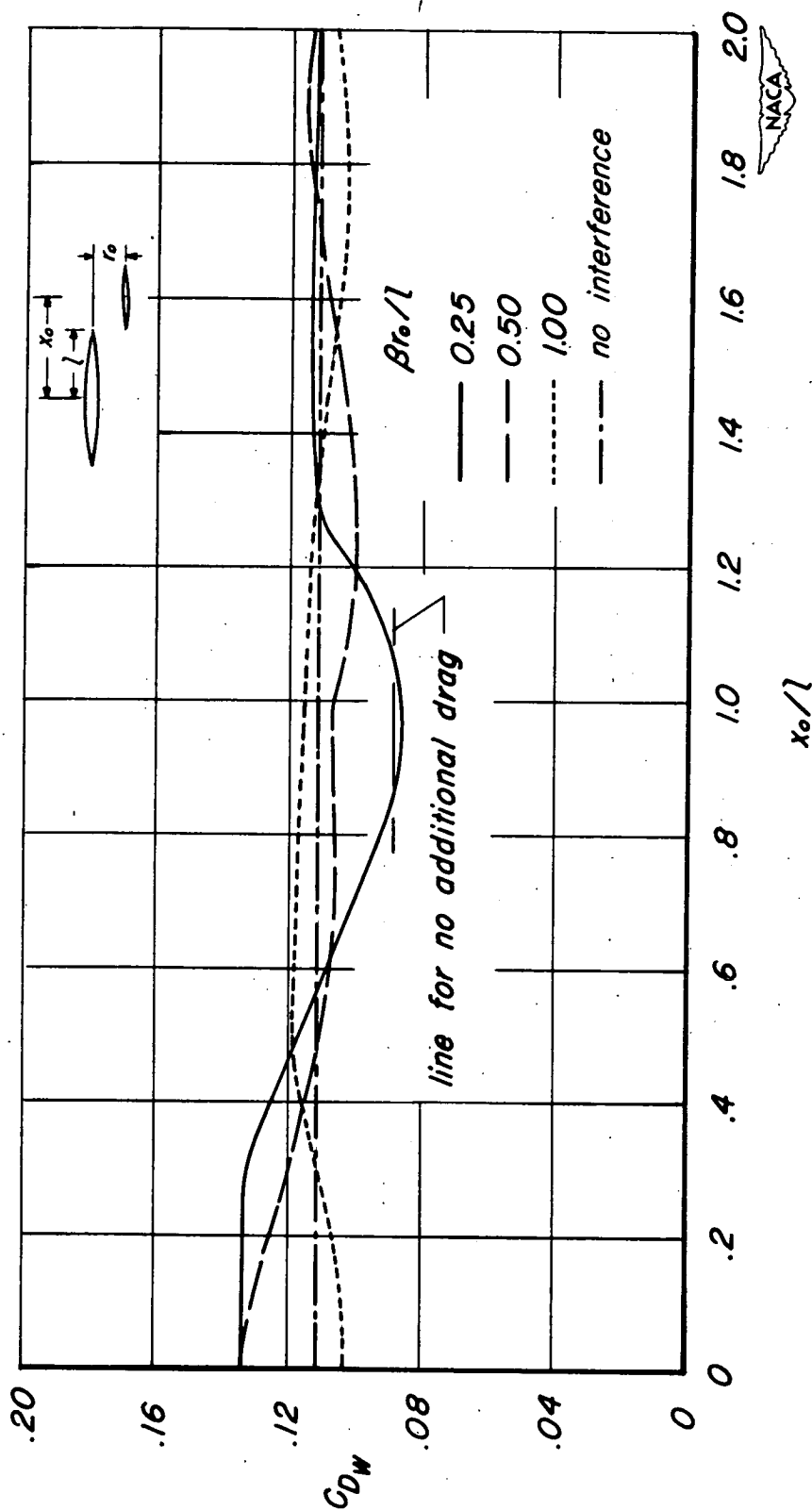


Figure 5. - Wave-drag coefficient of two-body systems based on total frontal area.

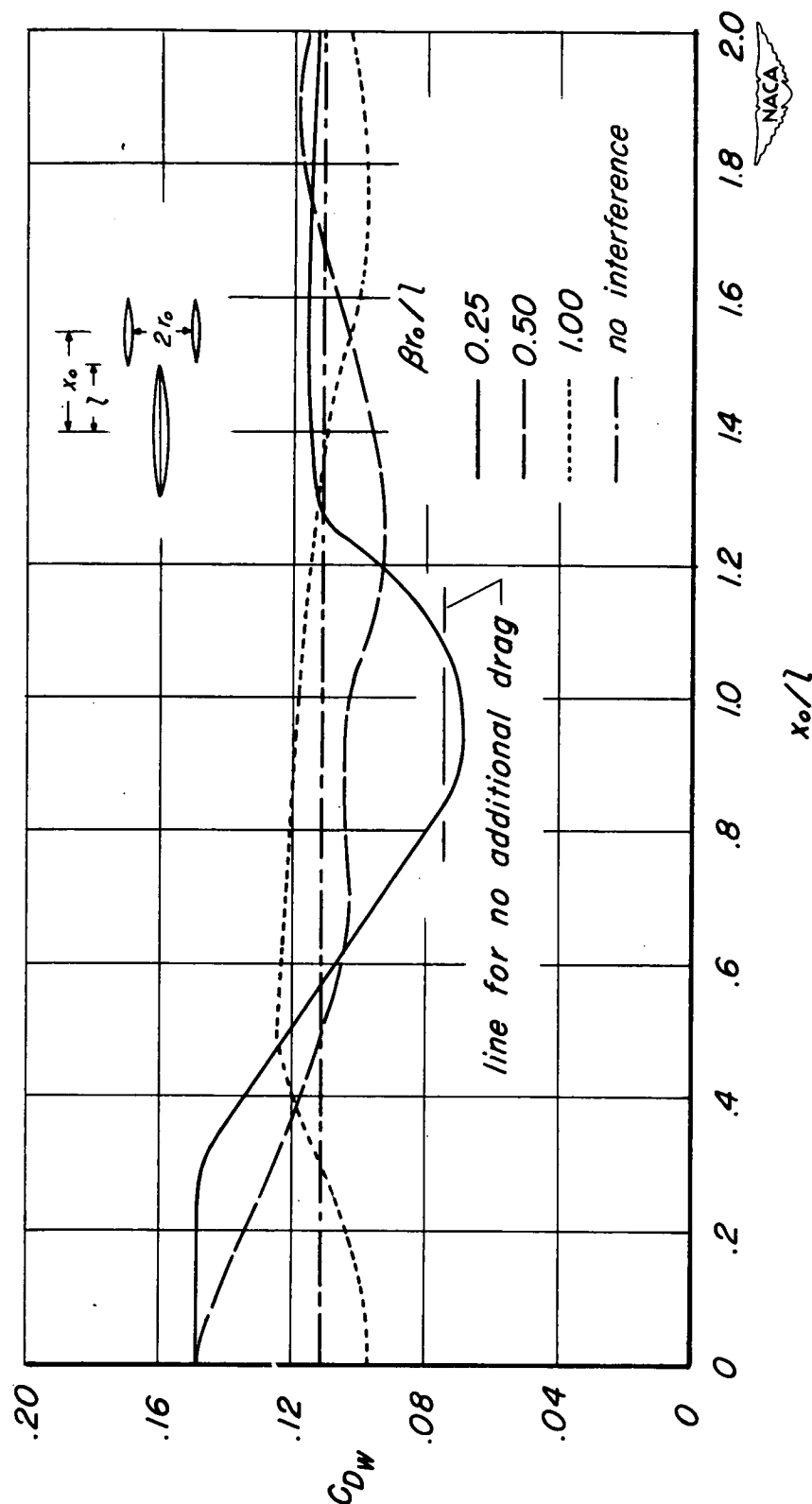


Figure 6.- Wave-drag coefficient of three-body systems based on total frontal area.